

University of Nebraska - Lincoln

DigitalCommons@University of Nebraska - Lincoln

---

C.J.G.J. Uiterwaal Publications

Research Papers in Physics and Astronomy

---

May 1995

## State-selected ion-molecule reactions: Statistical calculations with constraints

Cornelis J. Uiterwaal

*University of Nebraska - Lincoln, cuiterwaal2@unl.edu*

J. van Eck

*Utrecht University, 3508 TA Utrecht, The Netherlands*

A. Niehaus

*Utrecht University, 3508 TA Utrecht, The Netherlands*

Follow this and additional works at: <https://digitalcommons.unl.edu/physicsuiterwaal>

 Part of the [Physics Commons](#)

---

Uiterwaal, Cornelis J.; van Eck, J.; and Niehaus, A., "State-selected ion-molecule reactions: Statistical calculations with constraints" (1995). *C.J.G.J. Uiterwaal Publications*. 4.

<https://digitalcommons.unl.edu/physicsuiterwaal/4>

This Article is brought to you for free and open access by the Research Papers in Physics and Astronomy at DigitalCommons@University of Nebraska - Lincoln. It has been accepted for inclusion in C.J.G.J. Uiterwaal Publications by an authorized administrator of DigitalCommons@University of Nebraska - Lincoln.

# State-selected ion-molecule reactions: Statistical calculations with constraints

C. J. G. J. Uiterwaal,<sup>a)</sup> J. van Eck, and A. Niehaus

*Debye Institute, Department of Atomic and Interface Physics, Utrecht University, P.O. Box 80000, 3508 TA Utrecht, The Netherlands*

(Received 20 October 1994; accepted 21 February 1995)

For the two reactive systems,  $\text{NH}_3^+(E_{\text{int}}) + \text{NH}_3 \rightarrow \text{NH}_4^+ + \text{NH}_2$  and  $\text{H}_2^+(E_{\text{int}}) + \text{H}_2 \rightarrow \text{H}_3^+ + \text{H}$ , for which the relative cross sections were measured earlier in our group for  $E_{\text{c.m.}} \approx 40$  meV we calculated the relative cross section as a function of internal energy using the statistical Rice–Ramsperger–Kassel–Marcus (RRKM) theory that implicitly conserves total energy and total angular momentum. We found satisfactory agreement between theory and experiment by imposing rather mild constraints upon the loose transition state configuration. These constraints involve inactive vibrations and steric hindrance. The steric hindrance imposed in case of the  $(\text{NH}_3-\text{NH}_3)^+$  system is interpreted as being due to the anisotropic interaction of the ionic charge with the permanent electric dipole of the respective neutral collision partner in the two dissociation channels. We cannot be absolutely sure that the specific combination of modifications we propose for each of the two systems is the only one that agrees well with experiment. However, we find it striking that an agreement can be obtained by such weak and physically meaningful modifications, and we take this as a strong indication that the two studied systems do behave statistical. © 1995 American Institute of Physics.

## I. INTRODUCTION

It has been established many times in our group that a calculation of the relative cross section of state-selected ion-molecule reactions at thermal collision energies using the full statistical RRKM theory<sup>1–3</sup> in a simplified form fails to reproduce experimental data satisfactorily. However, agreement between experiment and theory could be found in many cases<sup>4–8</sup> by adapting an important parameter in the theory, namely the number of degrees of freedom that is taking part in the redistribution of internal energy. Therefore, we believe that for those systems where the number of degrees could be adapted with success the statistical assumption of rapid energy randomisation is essentially valid, but in a restricted sense: Apparently some dynamical constraints are playing a role. The model used in the references just given (see e.g. Ref. 4) serves as an ideal tool to find out if or if not some system behaves statistically, since it offers a simple parametrisation of the reaction cross section as a function of internal energy. Unfortunately, as a result of its simplicity, this model does not allow to extract any information about the nature of any possible dynamical constraints. Furthermore, this model does not take into account the conservation of angular momentum, which obviously is a dynamical constraint itself.

The purpose of the present paper is to show that the full statistical RRKM theory can be fruitfully extended to include some dynamical constraints, and that this procedure allows to some extent the identification of the nature of such dynamical constraints. The structure of this paper is as follows. In Sec. II a short overview of RRKM theory is presented, and in Sec. III we introduce two types of dynamical constraints. In Sec. IV we then demonstrate the usefulness of our

approach in a discussion of the following two reactions:



and



The relative cross sections for these reactions were measured earlier in our group,<sup>4,5</sup> for thermal collision energies ( $E_{\text{c.m.}} \approx 40$  meV). The cross section for reaction (2) was also measured by us at  $E_{\text{c.m.}} \approx 40$  meV as a spin-off of other work.<sup>9</sup> These results agree with the results of Ref. 4. Finally, some concluding remarks are given in Sec. V.

## II. RRKM THEORY

In this section we give a short resume of RRKM theory without constraints. Detailed descriptions of RRKM theory can be found in several texts.<sup>1–3</sup> For our calculations we used a FORTRAN code available from the Quantum Chemistry Program Exchange.<sup>10</sup> In RRKM theory, ion-molecule reactions are assumed to proceed via the formation of an intermediate collision complex. The formation of this complex is described by the well-known Langevin–Gioumousis–Stevenson (LGS) model.<sup>11,12</sup> In the context of this model, the capture cross section (or close collision cross section)  $\sigma_{\text{LGS}}$  for an ion (with charge  $q$ ) and a neutral molecule (with polarisability  $\alpha$ ) interacting through a  $-\alpha q^2/(2R^4)$  ion-induced dipole potential is given by

$$\sigma_{\text{LGS}} = \pi q \left( \frac{2\alpha}{E_{\text{kin}}} \right)^{1/2}, \quad (3)$$

where  $E_{\text{kin}}$  is the asymptotic kinetic energy in the center-of-mass system. In RRKM theory, the energy available to the complex is assumed to randomise rapidly over all degrees of freedom. Also, the overall reaction rate is assumed to be

<sup>a)</sup>Present address: FORTH–IESL, Laser and Applications Division, P.O. Box 1527, 71110 Heraklion, Crete, Greece.

controlled by the passage through a “bottleneck” or transition state. These two assumptions allow the probability for decay of the complex into some product channel  $j$  to be written as

$$P_j = \frac{W_j^\ddagger/S_j}{\sum_i W_i^\ddagger/S_i}, \quad (4)$$

where  $W_j^\ddagger$  is the sum of states available in the transition state configuration corresponding to product channel  $j$  with energy less than or equal to the total energy available. The quantity  $S_j$  is the symmetry number for channel  $j$ . (The QCPE program calculates sums of states without considering symmetry. Therefore, symmetry must be explicitly accounted for by the factor  $S_j$ .) In the present work, the transition states of all channels are assumed to be “loose” transition states, i.e., they are located at the top of the centrifugal barrier that arises at rather large distances as a result of the competition between the attractive  $-\alpha q^2/(2R^4)$  ion-induced dipole interaction and the repulsive  $L^2/(2\mu R^2) = E_{\text{kin}}(b^2/R^2)$  interaction caused by the centrifugal force ( $L$  = total angular momentum,  $b$  = impact parameter). For thermal collision energies, internal energy is not influencing the capture cross section, because the capture already takes place at a distance of typically 10 bohr, which is much larger than the typical size of the reactants. Also, because of the randomisation of energy, the intermediate complex will not “remember” the way it was energised. As a consequence, the two processes, formation of the complex plus its subsequent decay into products, can be considered as independent processes, related only through the conservation of total energy and total angular momentum. This implies that the cross section for reaction into channel  $j$  can be expressed as<sup>13</sup>

$$\sigma_j(E) = \int_{\text{all } J} dJ \frac{\partial \sigma_X(E, J)}{\partial J} P_j(E, J), \quad (5)$$

where  $\partial \sigma_X(E, J)/\partial J$  is the partial close collision cross section to form a complex with energy  $E$  and angular momentum  $J$  from the reactants. Making the usual assumption that the orbital angular momentum of the collision is much larger than the internal rotational angular momenta of the separated reactant molecules, this partial close collision cross section can be written as<sup>13</sup>

$$\frac{\partial \sigma_X(E, J)}{\partial J} = \begin{cases} \frac{\pi}{\mu E_{\text{kin}}} J & \text{if } J \leq L^* \\ 0 & \text{otherwise,} \end{cases} \quad (6)$$

where  $\mu$  is the reduced mass of the two reactants and  $L^*$  is the maximum orbital angular momentum given by

$$L^* = (8\alpha q^2 \mu^2 E_{\text{kin}})^{1/4}. \quad (7)$$

### III. RRKM CALCULATIONS WITH RESTRICTIONS

Two types of dynamical constraints will be of special interest to us here, namely incomplete vibrational relaxation and steric hindrance.

#### A. Incomplete vibrational relaxation

In its simplest form, RRKM theory assumes that the internal energy that is present in the collision complex immediately after its formation will rapidly randomise over *all* available degrees of freedom. This is not necessarily the case, however. The (small) coupling terms between the different degrees of freedom, such as anharmonic terms in the Hamiltonian, are responsible for this randomisation. If, for some transition state configuration, there exists a certain number of degrees of freedom that is insufficiently coupled to the reaction coordinate, the phase space available for intramolecular energy randomisation is effectively reduced. I.e., there exist regions of phase space that are not taking part in the energy randomisation, and the ensemble of points in phase space representing the starting conditions of the experiment does not flow into these isolated regions. (Assuming that the ensemble was initially outside these regions.) In that case, the sum of states for a given energy is reduced, and as a consequence the probability for reaction into the corresponding channel is decreased. This phenomenon can be simulated in our calculations by leaving out the uncoupled modes, i.e., for the calculation of the sum of states we use a reduced dataset in which some vibrations are removed, instead of a complete dataset containing all vibrations. If, for some system, a comparison with experimental data shows that a full statistical theoretical description (with a complete dataset of structural constants) does not give correct results, this type of vibrational phase space reduction can be applied. Of course, if two vibrational modes have a similar density of states, i.e., if they have approximately equal vibrational constants, leaving out the first one will give the same results as leaving out the second one. Therefore, the method described here is only able to discriminate between modes having largely different vibrational constants. The best approach is to divide the set of all vibrational constants into subsets with elements that are approximately equal to each other.

#### B. Steric hindrance

The rotational phase space can be reduced in reality because of steric hindrance, i.e., by a constraint on the relative orientation of the two fragments in the transition state configuration. This steric hindrance can be due to an orientation-dependent term in the interaction potential of the two fragments in the transition state configuration, which might “lock” the two fragments. It can also arise because there is not enough room for the two fragments to rotate freely without hindering each other geometrically. In Ref. 3 steric hindrance is discussed, together with some other examples of constrained rotations, such as torsional rotors and sinusoidally hindered rotors. In contrast to these other types of constrained rotations, steric hindrance can be included into our calculations in a straightforward manner. Therefore, steric hindrance is the only type of rotational constraint that we consider here. Because of steric hindrance, the vector describing the relative orientation of the two fragments cannot assume any direction anymore, but is confined to some solid angle  $\Delta\Omega$ . In a simple picture, we can imagine that the relative orientation vector can move freely inside this solid angle

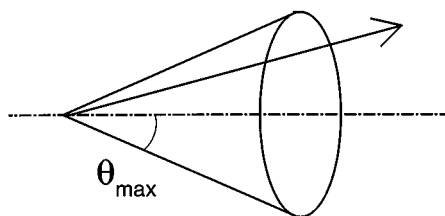


FIG. 1. Definition of the steric hindrance angle  $\theta_{\max}$ . The direction of the vector (shown as an arrow in the figure) describing the relative orientation of the two fragments in the transition state configuration is confined to the solid angle region that is defined by (using spherical coordinates)  $0 \leq \phi < 2\pi$  and  $0 \leq \theta \leq \theta_{\max}$ , and is shown as a cone (after Ref. 3).

$\Delta\Omega$ , and that for configurations with an orientation vector outside this solid angle the potential is high enough to make the rest of the  $4\pi$  solid angle that would be available for unhindered systems effectively inaccessible to the sterically hindered system. Reference 14 gives a simple method to include steric hindrance into the calculation of the rotational density of states. The effect of steric hindrance can be translated into our calculations by modifying the rotational constants. For a rotor having rotational constant  $B$  the effect of steric hindrance confining its orientation to a solid angle  $\Delta\Omega$  is correctly incorporated by using an effective rotational constant  $B_{\text{eff}}$  instead of  $B$ , given by

$$B_{\text{eff}} = \frac{4\pi}{\Delta\Omega} B. \quad (8)$$

If we assume that the solid angle  $\Delta\Omega$  is a cone consisting of the region defined by (using spherical coordinates)  $0 \leq \phi < 2\pi$  and  $0 \leq \theta \leq \theta_{\max}$ , as depicted in Fig. 1, the value of the hindrance angle  $\theta_{\max}$  is given by

$$\cos \theta_{\max} = 1 - 2 \left( \frac{B}{B_{\text{eff}}} \right). \quad (9)$$

Constraints on the rotations are to be expected for the  $(\text{NH}_3-\text{NH}_3)^+$  system, where the neutral partners in the two dissociation channels have permanent electric dipole moments which limit the rotational degrees of freedom due to the anisotropic charge-dipole interaction.

### C. Comparison of effects

We expect a qualitatively different effect resulting from a reduction of vibrational phase space as compared to reduction of rotational phase space. For a rotational degree of freedom, the energy levels are generally more closely spaced than for a vibrational degree of freedom. This is because the typical value of a rotational constant of  $\sim 10 \text{ cm}^{-1}$  (or  $\sim 1 \text{ meV}$ ) is much smaller than the typical value of a vibrational constant, which is  $\sim 1000 \text{ cm}^{-1}$  (or  $\sim 0.1 \text{ eV}$ ), so that in general rotational densities of states will be larger than vibrational densities of states. Also, the rotational density of states is influenced by the conservation of angular momentum, whereas the vibrational density of states is not. We therefore expect constraints imposed on vibrations and on rotations to have different effects.

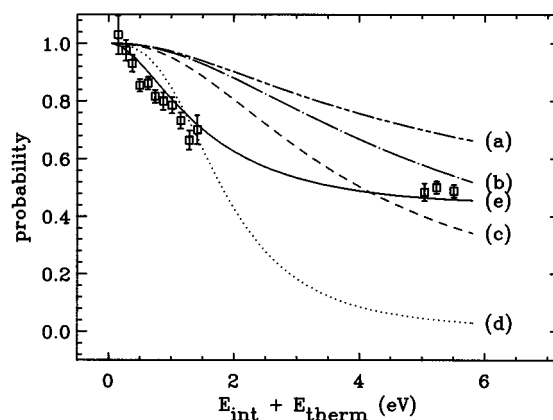
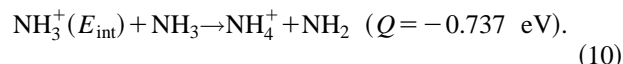


FIG. 2. Relative cross section (or reaction probability) of reaction (10) as a function of internal energy (including an amount of about 91 meV of thermal energy representing initial rotational and kinetic energy). The vertical axis gives the reaction probability, defined as  $P_j = \sigma_j / \sigma_{\text{LGS}}$  (see text). The squares are the experimental results of Ref. 5, scaled to fit the calculations. The five curves show the results of RRKM calculations with restrictions. (a) (dash-dot-dot curve) Result obtained when all degrees of freedom are active. (b) (dash-dot curve) One vibration of  $3420 \text{ cm}^{-1}$  in the products' transition state is inactive. (c) (dashed curve) One vibration of  $1330 \text{ cm}^{-1}$  in the products' transition state is inactive. (d) (dotted curve) Three vibrations of  $1330 \text{ cm}^{-1}$  in the products' transition state are inactive. (e) (solid curve) This is the result obtained for two inactive vibrations of  $1615 \text{ cm}^{-1}$  in the reactants' transition state and one inactive vibration of  $3420 \text{ cm}^{-1}$  together with increased rotational constants in the products' transition state:  $B_{\text{eff}}/B = 2.35$ , which implies  $\theta_{\max} = 81^\circ$ .

## IV. COMPARISON OF CALCULATIONS WITH EXPERIMENTAL RESULTS

### A. $\text{NH}_3^+ + \text{NH}_3 \rightarrow \text{NH}_4^+ + \text{NH}_2$

In this section we will discuss the results of RRKM calculations with constraints for the following reaction



Here,  $Q$  denotes the heat of reaction (the negative sign signals that the reaction is exothermal). The relative cross section of this reaction as a function of internal energy  $E_{\text{int}}$  of the reactant ammonia ion was measured earlier in our group.<sup>5</sup> These data are shown in Fig. 2. In these measurements, the ammonia ion was produced in two electronic states: the electronic ground state  $^2A_2'$  and the electronically excited  $^2E'$  state. The center of mass collision energy in these measurements was  $E_{\text{c.m.}} \approx 40 \text{ meV}$ . For internal energies above  $5.60 \text{ eV}$ , the primary ion  $\text{NH}_3^+(E_{\text{int}} > 5.60 \text{ eV})$  dissociates into  $\text{NH}_2^+ + \text{H}$ , so that only cross sections for  $E_{\text{int}} < 5.60 \text{ eV}$  could be measured. The total thermal energy in the system consists of a rotational part and a translational part, and is estimated to be  $E_{\text{therm}} \approx 90 \text{ meV}$ . The electronic energy of ammonia ions in the excited state  $^2E'$  is rapidly converted into vibrational energy of the electronic ground state by radiationless transitions.<sup>5</sup> Therefore, all measured cross sections can be considered as a single dataset concerning the electronic ground state of  $\text{NH}_3^+$ . As can be expected for exothermal reactions, the cross section decreases for increasing internal energy. For low internal energy, the sum of states for the backward channel is small, and the sum of

TABLE I. Parameters used in our RRKM calculations for reaction (10). The table gives unmodified parameters. Two channels were considered, indicated in the leftmost column, together with a characterisation of the moment of inertia (spherical, linear or atomic) of the two constituents of the channel. In the table,  $Q$  is the heat of formation with respect to  $\text{NH}_3^+ + \text{NH}_3$  both in their ground states,  $\mu$  is the reduced mass of the channel,  $\alpha$  is the polarisability of the neutral particle, the  $\omega$  are the vibrational constants of the channel, the  $B$  are the rotational constants of the channel, and  $S$  is the rotational symmetry number of the channel.

Channel <sup>a</sup> (pair type)	$Q$ (eV)	$\mu$ (amu)	$\alpha$ ( $\text{\AA}^3$ )	$\omega$ ( $\text{cm}^{-1}$ )	$B$ ( $\text{cm}^{-1}$ )	$S$
1. $\text{NH}_3^+ + \text{NH}_3$ (spherical- spherical)	0	8.50	2.26	3420(4)	7.64	18
				3325(2)	8.53	
				1615(4) 950(2)		
2. $\text{NH}_4^+ + \text{NH}_2$ (spherical- spherical)	-0.737	8.47	1.82	3420(3)	5.24	24
				3325	13.69	
				3230		
				3135		
				1615(2)		
				1520 1330(3)		

<sup>a</sup>All values are based on Ref. 17.

states for the forward channel is large. This implies that the probability for forward reaction is approaching unity. For increasing internal energies, the sum of states for the backward channel rapidly increases on a relative scale, so that the forward probability decreases.

In Fig. 2, curve (a) (dash-dot-dot-dot curve) is the result of a full statistical calculation (all degrees of freedom are active). The vertical axis shows the reaction probability, i.e., the fraction of the formed close collision complexes that decays into products (instead of decaying back into reactants again). The data used in this calculation are given in Table I. For the calculations we have neglected a possible influence of the charge-dipole interaction, like all other authors before.<sup>5,17</sup> Roughly speaking, one may distinguish two different types of influence, an influence on the formation of the collision complex, and an influence on its decay. The interaction potential  $V(R)$  between an ion and a point dipole at an intermolecular distance  $R$  is given by

$$V(R) = -\frac{\alpha q^2}{2R^4} - \frac{pq}{R^2} \cos \theta, \quad (11)$$

where  $\alpha$  is the polarisability of the neutral,  $q$  is the charge on the ion,  $p$  is the permanent dipole of the neutral and  $\theta$  is the angle between the centers of collision and the dipole axis. The influence on the formation of the complex can be estimated on the basis of the ADO model.<sup>21,22</sup> Using a permanent dipole moment for  $\text{NH}_3$  of  $p_{\text{NH}_3} = 1.47$  debye =  $4.90 \cdot 10^{-30}$  C · m = 0.578 atomic units, one estimates that the LGS cross section [Eq. (3)] has to be increased by about 40%. Since we do not calculate absolute cross sections this correction is irrelevant here. The increase of the upper limit of the total angular momentum [Eq. (7)], which is caused by a larger maximum impact parameter, amounts to 18%. This

increase is found to be insignificant for the calculations. The influence of the charge-dipole interaction on the decay of the complex, on the other hand, is expected to be much stronger, and difficult to access. We try here to account for this influence by introducing some steric hindrance into the Langevin model in the way described in Sec. III.

Figure 2 clearly shows that a full statistical description is incorrect. The same conclusion was drawn in Ref. 5, where the number of active degrees of freedom had to be decreased considerably to obtain agreement. These authors concluded that the reaction is statistical, although with some constraints. Other authors<sup>17</sup> had noticed earlier that the system does not behave as a full statistical model predicts, and they concluded that the reaction is nonstatistical. Our full statistical curve (a) is in qualitative agreement with the full statistical curves of Refs. 5 and 17, and is clearly in disagreement with the experimental points.

We obtained a satisfactory result [see curve (e) (solid curve) in Fig. 2] by excluding two out of 12 vibrations in the reactant channel ( $2 \times 1615 \text{ cm}^{-1}$ ) and one out of 12 vibrations in the product channel ( $3420 \text{ cm}^{-1}$ ), and by assuming steric hindrance in the product channel ( $B_{\text{eff}}/B = 2.35$ , or  $\theta_{\text{max}} = 81^\circ$ ). Thus, the conclusion in Ref. 5 that the reaction is statistical but with constraints is confirmed by our results. Remarkably, however, these authors concluded that the number of degrees of freedom had to be reduced by about<sup>18</sup> 83%, whereas we only have to reduce the number of degrees of freedom by about<sup>19</sup> 14%. Probably our method is better adapted to the problem, since, in contrast to the simple model used in Ref. 5, we include the conservation of angular momentum as a default constraint, and since we treat rotations and vibrations separately.

The other three curves in Fig. 2 show typical results that are obtained when exclusively vibrations are omitted but no rotational restrictions are assumed. Clearly, these curves are inconsistent with the experimental data, so that steric hindrance necessarily has to be assumed. [The vibrations we selected to be inactive are: for curve (b) (dash-dot curve) one vibration of  $3420 \text{ cm}^{-1}$  in the products' transition state; for curve (c) (dashed curve) one vibration of  $1330 \text{ cm}^{-1}$  in the products' transition state and for curve (d) (dotted curve): three vibrations of  $1330 \text{ cm}^{-1}$  in the products' transition state.]

The proposed steric hindrance in the dissociation channels is consistent with the experimental finding that internal energy is more effective in inhibiting the reaction cross section as the collisional energy is increased.<sup>20</sup> For the case that the ion-induced dipole interaction yields a good zero order description of the system within the statistical theory, we will demonstrate this below. Within the context of the statistical theory, the probability for reaction into some channel is proportional to the sum of accessible states in the transition state configuration of the channel. Here, we locate the transition states at the top of the centrifugal barrier. These so-called loose (or orbiting) transition states were described in Sec. II. For fixed asymptotic kinetic energy  $E_{\text{kin}}$  and polarisability  $\alpha$  the position  $R^\ddagger$  of the transition state configuration and the potential energy  $V^\ddagger$  in this configuration are given by (taking  $q=1$ )

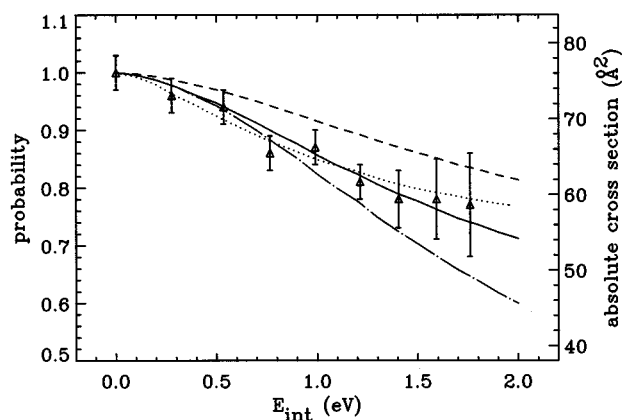


FIG. 3. Relative cross section (or reaction probability) of reaction (15) as a function of internal energy. The triangles are the experimental results of Ref. 4, and the dotted curve is a fit of these authors. Our best fit is shown as a solid curve; only steric hindrance in the product channel is assumed here. The dashed curve is the result of a full statistical calculation. Finally, the dash-dot curve shows the result for one inactive vibrational degree of freedom in the product channel of  $3178.29 \text{ cm}^{-1}$ . The LGS-RRKM formalism (see Sec. II) allows the calculation of absolute cross sections, given by the right-hand vertical axis.

$$V^\ddagger = \frac{b^4}{2\alpha} E_{\text{kin}}^2 \quad (12)$$

and

$$R^\ddagger = \frac{1}{b} \left( \frac{\alpha}{E_{\text{kin}}} \right)^{1/2}, \quad (13)$$

where  $b$  is the impact parameter. To allow the fragments to pass through the transition state configuration and thus to separate from each other, the height of the centrifugal barrier should be less than  $E_{\text{kin}}$ , the asymptotic kinetic energy (available for large distance between the fragments). Equation (12) implies that for a fixed value of  $E_{\text{kin}}$ , the resulting impact parameter of the two fragments can be in the range  $0 \leq b < (2\alpha/E_{\text{kin}})^{1/4}$ . The distance  $R^\ddagger$  between the two products in the transition state configuration is inversely proportional to this impact parameter as given by Eq. (13). Since for dissociating systems  $b$  cannot exceed  $(2\alpha/E_{\text{kin}})^{1/4}$  there is a lower limit on  $R^\ddagger$ , given by

$$R^\ddagger > \left( \frac{\alpha}{2E_{\text{kin}}} \right)^{1/4}. \quad (14)$$

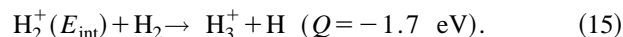
Equation (14) implies that the two products are closer together in the loose transition state configuration as more kinetic energy  $E_{\text{kin}}$  is deposited into the products. As a consequence, the products can be expected to experience more steric hindrance as the collision energy is increased.

We can only give a lower limit to the number of degrees of freedom that has to be modified. For example, if in both channels we exclude an extra vibration of  $3420 \text{ cm}^{-1}$ , the curve we find is not much different. The method we use is rather tedious for large systems, since one has to try out all possible combinations of active and inactive degrees of freedom to find a satisfactory one. While trying one readily notices, however, that the number of active degrees of freedom for the reactant and the product channel should not be too

much different, because if this is so, the probability for the channel with the largest number of active degrees of freedom equals unity over almost the whole energy range considered here. This limits the number of combinations that must be tried in practice.

## B. $\text{H}_2^+ + \text{H}_2 \rightarrow \text{H}_3^+ + \text{H}$

In this section we will discuss the results of RRKM calculations with restrictions for the following reaction



The heat of reaction  $Q$  of this exothermic reaction is given by Refs. 23 and 24. The relative cross section of this reaction as a function of internal energy  $E_{\text{int}}$  of the reactant hydrogen molecular ion was measured earlier in our group<sup>4</sup> for  $\text{H}_2^+(X;v=0-8)$ . These measurements are shown as triangles in Fig. 3. Recently, we also measured this cross section as a spin-off of other measurements.<sup>9</sup> The error in our measurements was larger than in the measurements of Ref. 4, although the two measurements are not significantly different. Therefore, in the discussion of restricted RRKM calculations on this reaction we will compare our calculated results with the earlier but more precise results of Ref. 4.

The result of a full statistical calculation on reaction (15) is shown in Fig. 3 as a dashed curve. The structural information used to calculate this curve is given in Table II. The best fit of Ref. 4 is shown as a dotted curve. Again we see that a full statistical calculation fails to agree with experiment. In this case we found agreement by adapting only the rotational constant of the  $\text{H}_3^+$ :  $B_{\text{eff}}/B = 1.59$ , or  $\theta_{\text{max}} = 105^\circ$ . This is the solid curve in Fig. 3. The vibrations are all active. If we select the vibrational mode with the largest vibrational constant ( $3178.29 \text{ cm}^{-1}$ ) to be inactive we obtain the dash-dot

TABLE II. Parameters used in our RRKM calculations for reaction (15). The table gives unmodified parameters. Two channels were considered, indicated in the leftmost column, together with a characterisation of the moment of inertia (spherical, linear or atomic) of the two constituents of the channel. In the table,  $Q$  is the heat of formation with respect to  $\text{H}_2^+(X;v=0) + \text{H}_2$ ,  $\mu$  is the reduced mass of the channel,  $\alpha$  is the polarisability of the neutral particle, the  $\omega$  are the vibrational constants of the channel, the  $B$  are the rotational constants of the channel, and  $S$  is the rotational symmetry number of the channel. Finally, the rightmost column shows the close collision cross section  $\sigma_{\text{LGS}}$  for the channel, calculated using Eq. (3) with  $E_{\text{kin}} = \frac{3}{2} kT$  and  $T = 300 \text{ K}$ .

Channel (pair type)	$Q^a$ (eV)	$\mu$ (amu)	$\alpha$ ( $\text{\AA}^3$ )	$\omega^b$ ( $\text{cm}^{-1}$ )	$B^c$ ( $\text{cm}^{-1}$ )	$S$	$\sigma_{\text{LGS}}$ ( $\text{\AA}^2$ )
1. $\text{H}_2^+ + \text{H}_2$ (linear-linear)	0	1.00	0.79	2321 4401.21	30.2 60.8530	4	76.1
2. $\text{H}_3^+ + \text{H}$ (spherical-atomic)	-1.7	0.75	0.67	2521.31 2521.31 3178.29	34.00	6	70.0

<sup>a</sup>Reference 23.

<sup>b</sup>Values for  $\text{H}_2^+ + \text{H}_2$  are from Ref. 15. Values for  $\text{H}_3^+ + \text{H}$  are quoted from Ref. 24.

<sup>c</sup>Values for  $\text{H}_2^+ + \text{H}_2$  are from Ref. 15. The  $\text{H}_3^+$  molecular ion has  $D_{3h}$  symmetry, so it is a symmetric top and two of its principal moments of inertia are equal. The single value for  $\text{H}_3^+ + \text{H}$  used here is the geometrical mean of the values for  $\text{H}_3^+$  as given by Ref. 16.

curve, which decreases too much as a function of internal energy. For the mode with the smaller vibrational constant ( $2521.31\text{ cm}^{-1}$ ) the resulting decrease is even faster.

As was the case for the reaction  $\text{NH}_3^+ + \text{NH}_3 \rightarrow \text{NH}_4^+ + \text{NH}_2$ , we can leave much more degrees of freedom intact than Ref. 4. To obtain agreement between theory and experiment we only have to modify one of the degrees of freedom, whereas in the more simple model of Ref. 4 it is necessary to reduce the fit parameter  $s$  considerably, from  $s=4.5$  and  $5$  for the reactant and the product channel respectively, to  $s=1.86$  and  $2.36 \pm 0.30$ .

## V. CONCLUSIONS

For two reactions of which the state-selected cross sections were measured earlier in our group we recalculated the cross section as a function of internal energy, using a model that implicitly conserves total energy and total angular momentum. We found satisfactory results by imposing rather mild constraints upon the transition state configuration. These constraints involve inactive vibrations and steric hindrance. We cannot be absolutely sure that the specific combination of modifications we propose for each of the two systems is the only one that agrees well with experiment. However, we find it striking that an agreement can be obtained by such weak modifications, and we take this as a strong indication that the two studied systems do behave statistical.

## ACKNOWLEDGEMENTS

This work is part of the research program of the "Stichting voor Fundamenteel Onderzoek der Materie (FOM)" which is financially supported by the "Nederlandse Organisatie voor Wetenschappelijk Onderzoek (NWO)."

<sup>1</sup>P. J. Robinson and K. A. Holbrook, *Unimolecular Reactions* (Wiley-Interscience, London, 1972).

- <sup>2</sup>W. Forst, *Theory of Unimolecular Reactions* (Academic, New York, 1973).
- <sup>3</sup>R. G. Gilbert and S. C. Smith, *Theory of Unimolecular and Recombination Reactions* (Blackwell, Oxford, 1990), and references therein.
- <sup>4</sup>D. Van Pijkeren, E. Boltjes, J. Van Eck, and A. Niehaus, *Chem. Phys.* **91**, 293 (1984).
- <sup>5</sup>D. Van Pijkeren, J. Van Eck, and A. Niehaus, *Chem. Phys.* **95**, 449 (1985).
- <sup>6</sup>D. Van Pijkeren, J. Van Eck, and A. Niehaus, *Chem. Phys.* **103**, 383 (1986).
- <sup>7</sup>C. E. Van der Meij, J. Van Eck, and A. Niehaus, *Chem. Phys.* **119**, 135 (1988).
- <sup>8</sup>C. E. Van der Meij, J. Van Eck, and A. Niehaus, *Chem. Phys.* **130**, 325 (1989).
- <sup>9</sup>C. J. G. J. Uiterwaal, J. Van Eck, and A. Niehaus, *J. Chem. Phys.* **102**, 744 (1995).
- <sup>10</sup>Quantum Chemistry Program Exchange, Program QCPE 557 TSTPST: Statistical Theory Package for RRKM/QET/TST/PST Calculations, QCPE Bulletin **8**, 137 (1988); code written by W. J. Chesnavich, L. Bass, M. E. Grice, K. Song, and D. A. Webb.
- <sup>11</sup>M. P. Langevin, *Ann. Chim. Phys.* **5**, 245 (1905).
- <sup>12</sup>G. Gioumousis and D. P. Stevenson, *J. Chem. Phys.* **29**, 294 (1958).
- <sup>13</sup>W. J. Chesnavich and M. T. Bowers, *J. Am. Chem. Soc.* **98**, 8301 (1976), and references therein.
- <sup>14</sup>S. W. Benson, *Thermochemical Kinetics*, 2nd ed. (Wiley, New York, 1976), as cited by Gilbert and Smith (1990).
- <sup>15</sup>K. P. Huber and G. Herzberg, *Molecular Spectra and Molecular Structure IV. Constants of Diatomic Molecules* (Van Nostrand, Toronto, 1979).
- <sup>16</sup>T. Oka, *Phys. Rev. Lett.* **45**, 531 (1980).
- <sup>17</sup>W. J. Chesnavich and M. T. Bowers, *Chem. Phys. Lett.* **52**, 179 (1977).
- <sup>18</sup>Actually, they did not consider the number of degrees of freedom directly, but an exponent  $s$ , which is closely related to the number of degrees of freedom. If all degrees of freedom are active, the expected value for this exponent is 15.5; instead they found  $s=2.71 \pm 0.47$ .
- <sup>19</sup>For each of the two channels, we modified 2 of the 14 available degrees of freedom (12 vibrational plus 2 rotational), so the reduction is  $2/14 \approx 14\%$ .
- <sup>20</sup>T. Baer and P. T. Murray, *J. Chem. Phys.* **75**, 4477 (1981), as cited by Van Pijkeren *et al.* (1985).
- <sup>21</sup>T. Su and M. T. Bowers, *J. Chem. Phys.* **58**, 3027 (1973).
- <sup>22</sup>M. T. Bowers and T. Su, in *Interaction between Ions and Molecules*, Nato Adv. Study Inst. Ser. **B6**, edited by P. Ausloos (Plenum, New York, 1975).
- <sup>23</sup>T. R. Hogness and E. G. Lunn, *Phys. Rev.* **26**, 44 (1925), as cited by Lie and Frye (1992).
- <sup>24</sup>G. C. Lie and D. Frye, *J. Chem. Phys.* **96**, 6784 (1992).